Island topographies to reduce short-circuiting in stormwater detention ponds and treatment wetlands

TITLE: Island Topographies to Reduce Short-Circuiting in Stormwater Detention Ponds and Treatment Wetlands

Accepted: Journal of Ecological Engineering 2018

AUTHORS

Celina Balderas Guzman[1], Samantha Cohen[2], Manoel Xavier[3], Tyler Swingle[4], Waishan Qiu[2], Heidi Nepf[3*]

* corresponding author

[1]Norman B. Leventhal Center for Advanced Urbanism, School of Architecture & Planning, Massachusetts Institute of Technology, Cambridge, MA 02139, USA

[2]Department of Urban Studies and Planning, Massachusetts Institute of Technology, Cambridge, MA 02139, USA

[3]Department of Civil and Environmental Engineering, Massachusetts Institute of Technology, Cambridge, MA 02139, USA hmnepf@mit.edu.

[4]Department of Architecture, Massachusetts Institute of Technology, Cambridge, MA 02139, USA

ABSTRACT

Urban stormwater is an increasing environmental problem for cities worldwide. Many cities have turned to green infrastructure solutions, which provide water treatment and retention while also harnessing other ecosystem services. This study considered the design of detention ponds and treatment wetlands with the goal of improving hydraulic performance (specifically reducing short-circuiting) while also increasing habitat diversity. Fifty-four basin topographies, including a variety of islands and berms, were compared to an open and a traditional serpentine basin. Using scaled physical models the hydraulic performance of each design was evaluated using tracer studies to construct the residence time distribution and to visually observe the circulation pattern. In addition, the earthwork construction cost and habitat diversity index (based on the Shannon-Weaver entropy measure) were estimated at field scale. The results reveal multiple design options that improve hydraulic performance, relative to both the open and serpentine basins, and which represent a range of habit diversity and cost. General guidelines for optimal configurations are discussed.

HIGHLIGHTS (85 characters max per bullet point, 3-5 bullet points)

- Island clusters near inlet improve hydraulic performance of detention ponds and wetlands
- The number, size, shape, and placement of islands impacts hydraulic performance
- Islands add habitat diversity by creating depth heterogeneity and upland area
- Island design options exist with high performance and variable earthwork volume

KEYWORDS (max 6)

stormwater detention ponds, treatment wetlands, residence time, green infrastructure design

1. INTRODUCTION

Urban stormwater is an increasing environmental problem for cities worldwide. In the United States today, stormwater impairs 97,300 km of rivers, 3100 m^2 of lakes, and 16,900 km^2 of bays and estuaries (U.S. EPA, 2017). Urban stormwater is a growing source of water pollution, and the number of natural ecosystems impaired by stormwater continues to rise (U.S. EPA, 2015). Cities depend on these ecosystems for critical services, such as climate regulation, noise reduction, air purification, and flood protection (Gómez-Baggethun et al., 2013). The latter is especially important given that climate change will bring storms of increasing intensity, posing greater flood risks (Walsh, 2014). To address this challenge, many cities have turned to green infrastructure, such as bioswales, green roofs, detention ponds, and treatment wetlands, to capture and treat stormwater. Green infrastructure often has at a lower cost than traditional infrastructure, while providing ancillary ecological and social benefits (Lovell and Johnston, 2009; Rousseau et al., 2008; Moore and Hunt 2012, 2013; U.S. EPA, 2015; Atkins, Inc., 2015; Connop et al., 2016). This paper considers landscape designs for detention ponds and treatment wetlands that offer opportunities to provide habitat and re-introduce nature into cities (Worrall et al., 1997; Connor and Luczak, 2002; Ghermandi and Fichtman, 2015).

Habitat heterogeneity supports biodiversity, which underlies the provision of ecosystem services (Elmqvist et al., 2013). Research on treatment wetlands has shown that heterogeneity in landscape is the key to creating habitat. The EPA recommends eschewing rectangular basins in favor of sinuous edges and using varied slopes and grades to create different water depths (U.S. EPA, 2000), which is also echoed by Worrall et al. (1997). Other researchers have noted the contribution of topography in constructed wetlands to habitat diversity and species richness (Vivian-Smith, 1997; Sleeper and Ficklin, 2016). In mitigation wetlands, micro-topography has been shown to aid nitrogen cycling and removal (Wolf et al., 2011).

To function best, the flow in a detention pond or constructed wetland should approach plug flow, in which all of the water entering the system remains for the nominal residence time,

$$T_n = V/Q, \tag{1}$$

with V the system volume and Q the inflow rate. However, in most situations, plug flow is not achieved, and short-circuiting of flow between the inlet and outlet occurs. In shallow basins, short-circuiting is associated with asymmetric circulation patterns that grow from instabilities at the inflow (Dewals et al., 2008; Dufresne et al., 2010). In vegetated regions, short-circuiting may be promoted by heterogeneous distributions of vegetation or by channels cutting through vegetation (Dierberg et al., 2005; Lightbody et al., 2008). Short-circuiting undermines the performance of a pond or wetland by allowing much of the water to exit in less than T_n. Many of the biochemical, filtering, and settling processes that reduce pollutant levels are first-order reactions, for which the highest rates of reduction ($\partial C/\partial t$) occur at early time. Therefore, water parcels leaving at times shorter than the design time, i.e. short-circuiting, achieve significantly less reduction in concentration than parcels leaving at the design time.

Because of its adverse effects, engineers have devoted substantial research to identify basin geometry that reduces or eliminates short-circuiting. For example, short-circuiting is reduced in basins with long aspect ratio (Thackston et al., 1987) or with sinuous channels or baffles (Farjood et al., 2015; Savickis et al., 2016). In treatment wetlands, the insertion of unvegetated deep zones perpendicular to the flow path has been shown to counter-act the short-circuiting associated with channels that cut through vegetated regions (Lightbody, 2007). Other studies have suggested islands to deflect inflow and improve the circulation pattern within treatment wetlands and ponds (German and Kant, 1998). Persson et al. (1999) tested 13 pond designs, including 2 with islands, using MIKE21, a depth-averaged numerical model. They found that the scenario with an island at the inlet reduced short-circuiting, compared to a basin with no island or with berms (Persson et al., 1999; Persson, 2000). In 2004, Adamsson et al (2002) physically modeled a square island near the inlet, considering islands with edges parallel and rotated 45 degrees to the basin edges. The addition of the island decreased short-circuiting, with the greater benefit from the parallel island than the rotated island (Adamsson et al., 2002). In contrast, Khan et al. (2011) found that the addition of an island (either parallel or rotated) increased short-circuiting and decreased the performance of a scaled detention pond model. Khan attributed the poor performance to the sloping walls of the narrow basin, which created shallow regions through which inflow short-circuited around the island. The Khan and Adamsson studies together suggest that the potential impact of a deflector island is sensitive to the size of the island, the position within the basin and the basin geometry. Therefore, while some promising results have been reported for islands, additional studies are needed to identify the optimum island designs. This paper expands on previous research by exploring more complex island topographies, using the open basin and serpentine design for comparison. Each design was evaluated for hydraulic performance, habitat diversity, and earthwork cost.

2. EXPERIMENTAL METHODS

Experiments were conducted in two phases. In the first phase, a set of simple geometric shapes were cast in concrete and used to create 20 basic wetland configurations (Figure 1), including berms, islands, and pinch points, which are constrictions that separate the basin into two sub-basins. The results of phase 1 indicated that a cluster of islands near the inlet provided the greatest hydraulic improvement, so that phase two of the experiments focused only on islands, constructed with greater topographic detail. Specifically, phase 2 included 34 designs, exploring different number, size, shape, and placement of islands (Fig. 2). In both testing phases, the hydraulic performance was evaluated using tracer studies to estimate the residence time distribution and associated metrics (Section 2.2). In addition, the earthwork construction cost and habitat diversity were estimated for each of the topographies at field scale (Sections 2.3 and 2.4).

2.1 Physical Models

The first phase of experiments used a scaled model of the detention basin described in Khan et al. (2013), designed with the Froude number scaling detailed in Shilton (2001). The model basin measured 120 cm by 40 cm and had sloped sides, with a 1-cm inlet and outlet centered 1 cm above the bed. The water depth was $H = 3.0 \pm 0.1$ cm, which was sufficient to avoid surface tension affects (Shilton 2001). With a flow rate of $Q = 4.8 \times 10^{-5}$ m^3/s, the nominal residence time for the open basin (which was considered the control, denoted with sub-script '*nc*') was $T_{nc} = 300 \pm 10$ s. Concrete shapes were placed inside the basin to create 20 basic configurations of berms, island clusters, and pinch points (Figure 1).

In the second phase, 34 island topographies were tested, including islands of different number, size, shape, and placement, as well as an open basin and a serpentine design (Figure 2). These topographies were designed in Rhinoceros, a 3D computer-aided design (CAD) program, and robotically milled out of high-density foam using a CNC machine. Each model measured 40.5 cm wide and 60 cm long. Relative to the full-scale prototype, the model height was exaggerated by a factor of two to avoid surface tension effects. For ease of fabrication, the islands were made with flat faces.

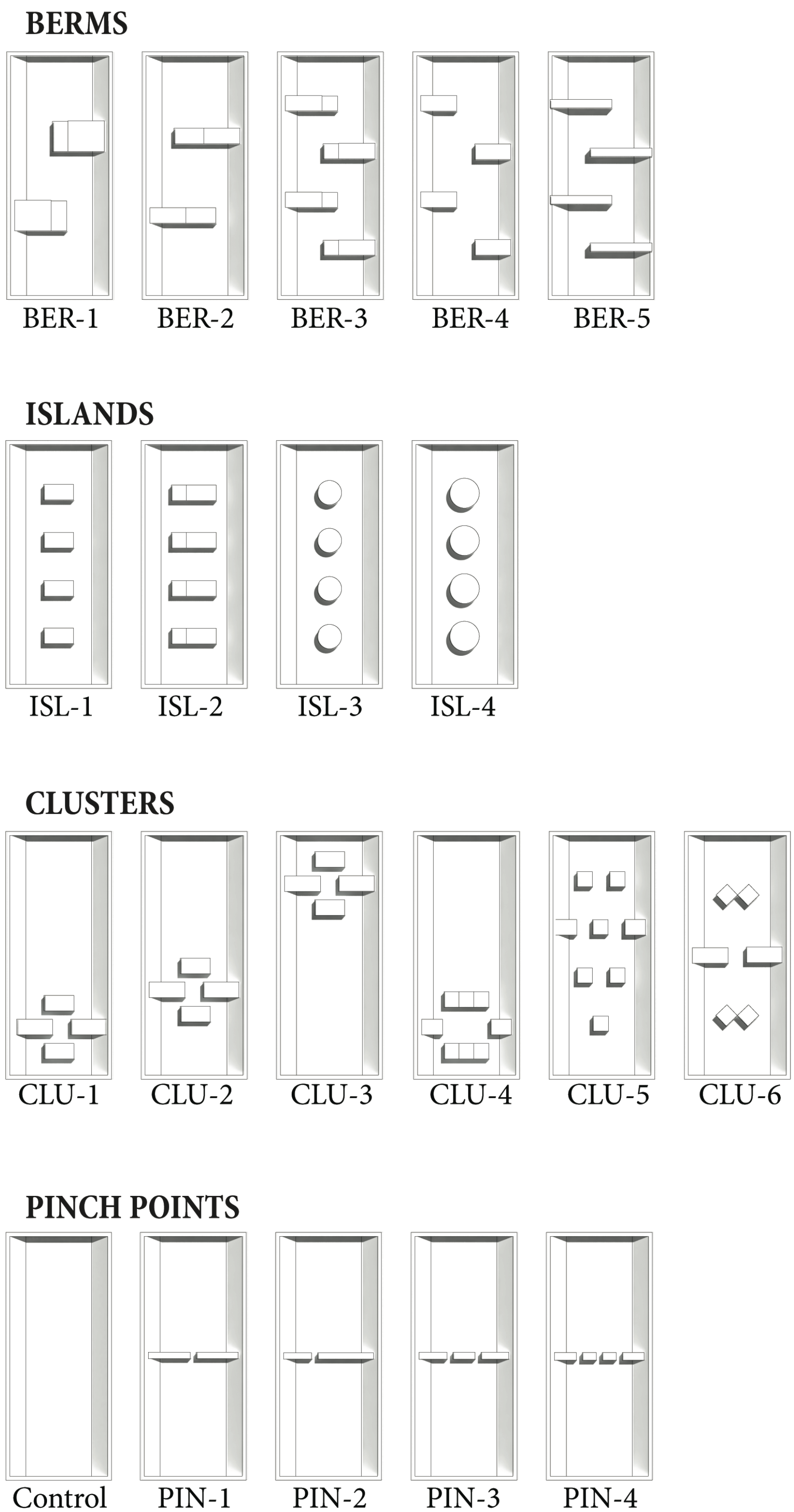

Figure 1. Top view of the phase 1 experimental basins, each 120 cm by 40 cm and with sloped sides. Flow is from bottom to top in each schematic.

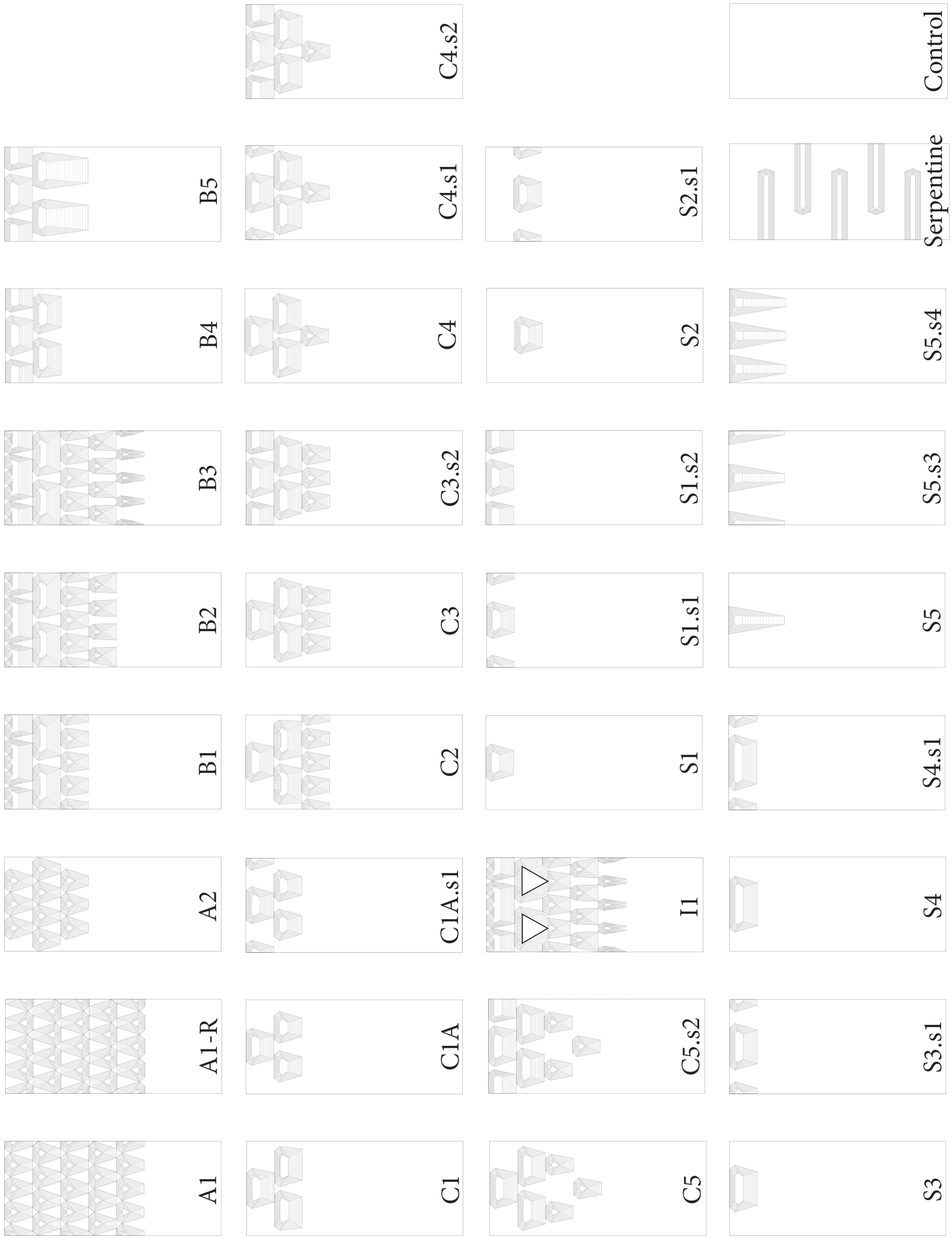

Figure 2. Top view of phase 2 topographies, 40.5 cm wide and 60 cm long. Flow was from left to right. The dimensions of each island are provided in a supplemental file.

The model topographies were placed in a plexiglass flume measuring 3.75 m long and B = 0.41 m wide (Figure 3). Downstream of each topography, a flat bed was added to create a test basin of length L = 93.0±0.2 cm. The topographies were attached to a concrete base to prevent floating. The flume was filled to a water depth of H= 3.3 ± 0.2 cm over the model. A variable speed pump provided a discharge of 0.200 ± 0.011 L s^{-1}. To produce a straight inflow, flow entered the test basin through a 28-cm long inlet channel with the same width as the basin inlet, 2.2 cm. The outlet was 3 cm wide to accommodate the fluorometer. The Reynolds number of the inflow was $Re = Uh/\nu = 9000$, with U the inflow velocity and ν the kinematic viscosity. Consequently, the circulation pattern was inertia-dominated and should be representative of the flow field at full-scale. For the phase 2 experiments, the nominal residence time of the open basin, which was used as a control, was T_{nc} = 63 ± 3 s, (with subscript "c" denoting control). The uncertainty reflects the variation in flow rate. Two replicate experiments were conducted for each of the topographies.

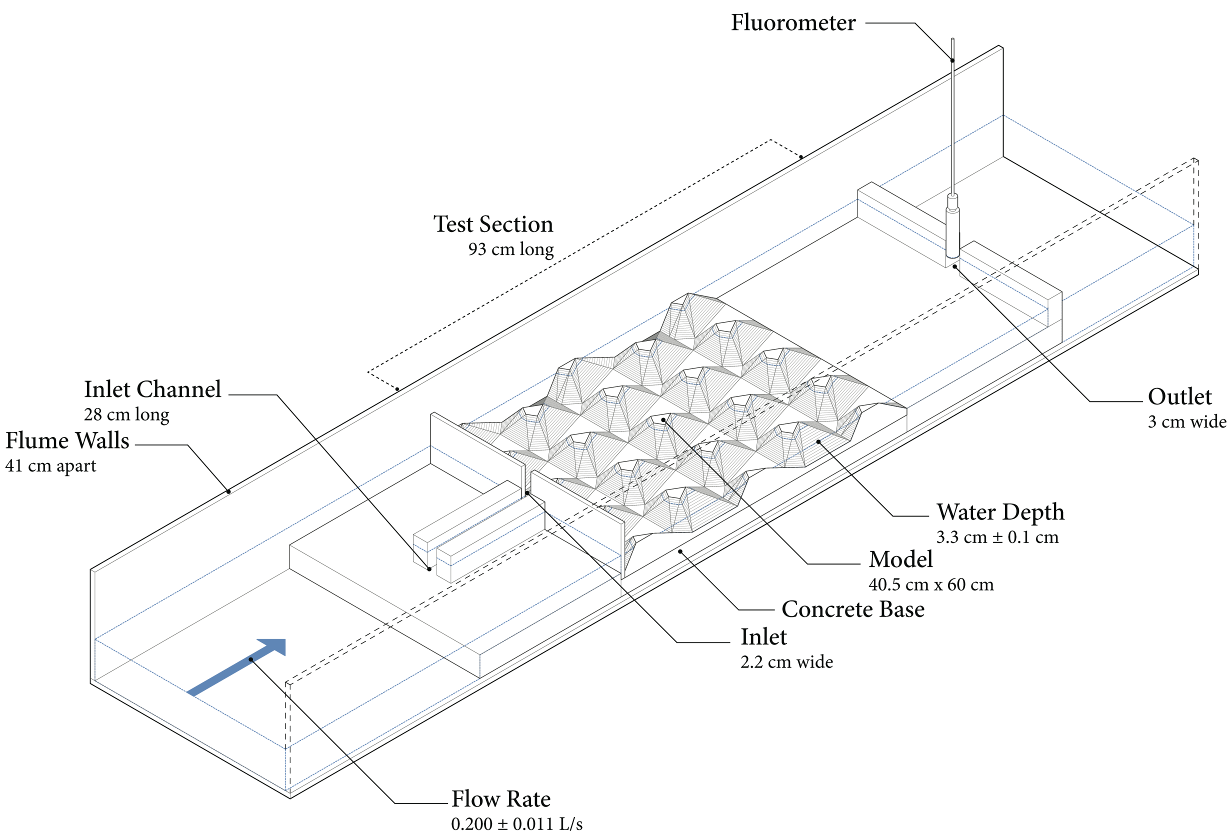

Figure 3. Experimental set-up with island topography A1, which had five rows of islands.

2.2 Tracer Testing and Hydraulic Performance Metrics

The residence time distribution of each design was measured using a standard tracer experiment. A 1 mL slug of 1:10,000 rhodamine solution was injected over less than 1 second into the inlet channel. The concentration of tracer at the outlet, C, was measured as a function of time since release, t, using a UniLux fluorometer sampling at 1 Hz. To adequately capture the tail of the distribution, the concentration was measured for four times the nominal residence time of the open basin, $4T_{nc}$. The residence time distribution (RTD) was estimated from the concentration recorded at the outlet (e.g., Werner and Kadlec, 1996):

$$RTD\,(t) = \frac{QC(t)}{\int_0^{\infty} QC(t)dt} \tag{2}$$

Two metrics were used to compare the performance of the different topographies. First, short-circuiting is associated with mass leaving the basin at times much shorter than the nominal residence time, so that a reasonable metric for short-circuiting is the time at which 10% of the injected mass has exited the basin, which was called T_{10}. To account for the loss of volume associated with the inclusion of topography, which shortens the nominal residence time, T_{10} was normalized by the nominal residence time of the open basin control, T_{10}/T_{nc}. Second, assuming a pond was operated at steady-state conditions with inflow concentration C_o and exit concentration C_e, the expected pollutant removal efficiency can be defined as C_e/C_o (e.g., Kadlec and Wallace, 2009). Assuming pollutant removal follows a first-order reaction, with rate constant k,

$$\frac{C_e}{C_0} = \int_0^{\infty} RTD(t)\exp(-kt)\,dt \tag{3}$$

For a consistent comparison, the rate constant was set to $k = 1/T_{nc}$ for all cases.

Two replicates were conducted for each basin topography, yielding two estimates of T_{10} and C_e/C_o. Table 3 reports the mean of the replicates and the uncertainty, defined using the standard error (SE), which for two replicates is ½ the difference between replicates (e.g. Taylor, 1997). The uncertainty was taken to be 1.96 SE for 95% confidence. In some cases the replicate T_{10} values were identical, yielding $SE = 0$, for which the uncertainty was defined by ½ the sampling resolution (0.5 s). The variation in flow rate was the main contributor to the uncertainty in estimated T_{nc} (δT_{nc} = 3 s). The uncertainties δT_{10} and δT_{nc} were combined to produce the uncertainty in the metric T_{10}/T_{nc} (Taylor, 1997),

$$\frac{\delta(T_{10}/T_{nc})}{(T_{10}/T_{nc})} = \sqrt{\left(\frac{\delta T_{10}}{T_{10}}\right)^2 + \left(\frac{\delta T_{nc}}{T_{nc}}\right)^2} \quad (4)$$

Finally, streamline maps were constructed using a frame-by-frame analysis of digital video. Tracer was sequentially injected at multiple points within the basin to trace out different streamlines. The upstream movement of tracer identified regions of recirculation. Specifically, the boundary of a recirculating region was located where injections of tracer transitioned from being carried upstream (in a recirculation zone) to downstream (outside a recirculation zone).

2.3 Construction Cost

The earthwork costs (excavation, rough grading, and fine grading) were used to compare differences in construction cost between the topographies. The costs that would be the same for all topographies are intentionally excluded, e.g. the removal of excess soil and site preparation (e.g. clearing and grubbing, managing difficult soils, or dewatering). We also excluded site-dependent costs, such as erosion control measures and maintenance costs. The earthwork costs were estimated for a field-scale basin 21 m wide and 47 m long and operated at a water depth of 0.8 m. The earthwork costing methodology was developed with assistance from Mark Lindley, PE, Senior Engineer at Environmental Science Associates. The earthwork costs assumed the wetland and islands were constructed below grade, requiring excavation and grading of soil. The soil volume removed to form islands was multiplied by excavation cost outlined in the RSMeans cost manual (2017) (Table 1). After excavation, two passes of rough grading shaped the islands. The surface area of each island was multiplied by the rough grading cost per area. Finally, the cost of one pass of finish grading was calculated based on the surface area of the entire site.

2.4 Habitat Diversity

The habitat diversity index (*H*) was calculated using the Shannon-Weaver entropy measure (Shannon and Weaver 1949, Krebs 2009), which other researchers have used for the same purpose (Kearney et al. 2013, Brandt et al. 2015). Using water depth as a proxy for habitat, we measured the topographical surface area that fell into each of four habitats: upland (above water), emergent vegetation (0 to 30 cm water depth), submerged vegetation (30 cm to 46 cm water depth), and open water (deeper than 46 cm). As with the construction cost, this index was calculated for each design at full scale. For N habitat zones, the habitat diversity index is

$$H = -\sum_{i=1}^{N} p_i \ln(p_i) \tag{5}$$

in which p_i is the proportion of total area occupied by the ith habitat zone (e.g. Kearney et al., 2013). The maximum habitat index is

$$H_{max} = ln\,(N), \tag{6}$$

so that for $N = 4$ habitats, $H_{\max} = 1.39$. The minimum value was zero, corresponding to the control because it had only one habitat zone (open water).

3. Results and Discussion

3.1 Phase 1

The first phase of experiments compared simple bathymetric features (baffles, island clusters, and pinch points), using the short-circuiting parameter T_{10}/T_{nc} (Table 2). For the open basin control $T_{10}/T_{nc} = 0.22 \pm 0.06$. This value reflected the presence of significant short-circuiting between the inlet and outlet. In some cases, the addition of topography made short-circuiting worse ($T_{10}/T_{nc} < 0.22$). In particular, every case with islands distributed along the centerline (ISL-1 to ISL-4, Figure 1) produced a lower metric, with $T_{10}/T_{nc} < 0.17$. In these cases, although the initial island deflected the inflow, which should diminish short-circuiting, the series of islands created channels along the basin edges, which became new regions of short-circuiting. This was similar to the enhanced short-circuiting observed by Khan et al (2011) for a detention pond with a single central island.

The serpentine bathymetries (BER-1 to BER-4, Fig. 1) mostly improved the hydraulic performance, consistent with previous recommendations (e.g. Thackston et al., 1987). The exception was BER-4, with baffles that did not extend past the basin centerline, and thus did not block the inlet-outlet short-circuiting path. In this case, the performance metric was $T_{10}/T_{nc} = 0.20 \pm 0.04$. In contrast, with the same basic geometry as BER-4, but longer baffles, BER-3 produced T_{10}/T_{nc} = 0.31±0.04, demonstrating the importance of extending baffles past the basin centerline.

The pinch point series was inspired by the idea of breaking a single basin into two basins in series, which, based on tanks-in-series analysis (e.g. Fogler, 1992; Kadlec and Wallace, 2009), should improve hydraulic performance. Generally, the pinch point cases did better than the open basin, but none were top performers. The top performers, CLU-4 and CLU-1, both included island clusters located at the inlet, with T_{10}/T_{nc} = 0.38±0.04 and 0.51±0.05, respectively. These cases performed well because the first island split the inflow jet into two segments, and subsequent islands met and deflected each of the jet segments, spreading the inflow over the basin width. Because the island clusters produced the highest values of T_{10}/T_{nc}, the second phase of experiments considered more complex island clusters at the inlet.

3.2 Hydraulic Performance of Phase 2 Topographies

In the second phase, 34 topographies were tested, including an open basin and a serpentine basin for comparison. The estimated metrics for all topographies are listed in Table 3. Based on the short-circuiting metric, T_{10}/T_{nc}, all of the island designs improved performance compared to the control (Figure 4a). Moreover, 23 cases produced lower values of T_{10}/T_{nc} than the serpentine design. The best performing designs were C1A.s1, which had 2 rows of similar islands, and I1, which had 5 rows of islands that decreased in size with distance from the inlet (Figure 2). Both designs achieved T_{10}/T_{nc}= 0.57±0.03. Recall that for ideal plug flow, T_{10}/T_{nc} = 1. However, this cannot be achieved with island topographies, because the addition of islands reduces the available volume, so that the effective T_n is less than T_{nc}. It is difficult, without more extensive testing, to determine the upper limit of feasible T_{10}/T_{nc} values. However, the results here do show that improvements over an open basin can be achieved with the addition of islands. Ultimately, the degree of engineering intervention selected to improve the performance of a given basin will depend on the constraints of cost and required concentration reduction.

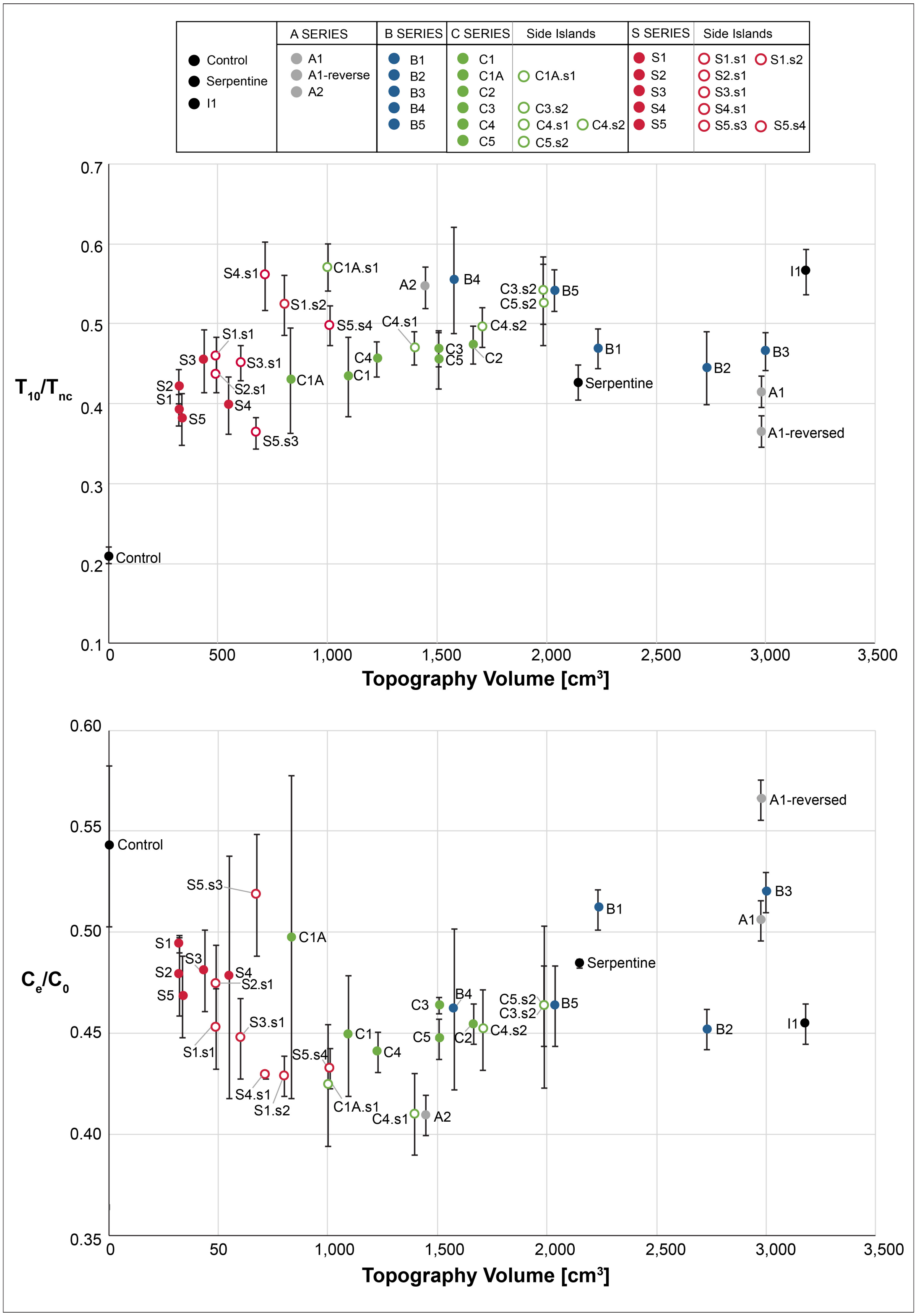

Figure 4 Performance metrics vs topography volume in scaled model. (a) T_{10}/T_{nc}, metric for short-circuiting. (b) C_e/C_o, pollutant removal efficiency from eq. 4 and assuming rate constant $k = 1/T_{nc}$. Error bars indicate 95% confidence interval based on two replicates and the propagated uncertainty in T_{nc}.

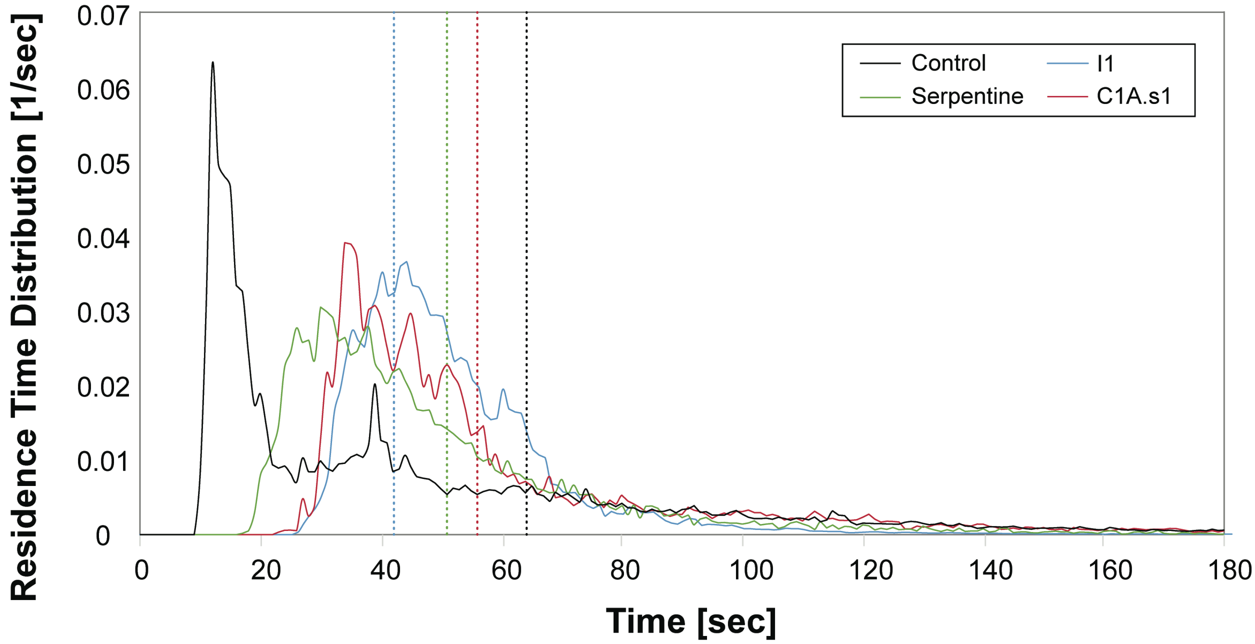

Figure 5. *RTD* for control (black) and serpentine (green) cases, and for the island cases with highest T_{10}/T_{nc}, specifically I1 (blue) and C1A.s1 (red). Each *RTD* is the average of two replicates. The nominal residence time of each case, which accounts for water volume lost to island volume, is located at the vertical line of matching color.

Figure 5 compares the *RTD* for the best performing cases (I1 and C1A.s1) to the control and serpentine cases. A vertical line of matching color shows the nominal residence time of each case. When short-circuiting was present, the *RTD* peak occurred before the nominal residence time. The greatest short-circuiting occurred in the open basin (black curve in Fig. 5), with the *RTD* peak occurring long before the nominal residence time (vertical black line). The time between the peak and nominal residence time decreased for the serpentine (green) and C1A.s1 (red). The case with 5 rows of islands (I1, blue curve) was closest to plug flow, with the *RTD* peak arriving at its nominal residence time. For I1 the islands decreased in size with distance from the inlet, which smoothly spread the inflow to a laterally-uniform distribution at the end of the island sequence. Note that while similar performance was achieved by C1A.s1 and I1, both with T_{10}/T_{nc}= 0.57±0.03, I1 required more than twice the earthwork volume, showing that designers have choices amongst high-performing cases with more or less earthwork, which would have different impacts on construction cost, habitat creation, and storage volume.

Next, we considered how the difference in hydraulic performance translated into pollutant removal, indicated with C_e/C_o (Figure 4b), assuming a first-order reaction with rate constant $k = 1/T_{nc}$. All of the island topographies, except for A1-reversed, produced values of C_e/C_o lower than the control (0.54±0.04). Most of the topographies produced lower values than the serpentine (0.484±0.002). Generally, cases with higher T_{10}/T_{nc} (Figure 4a) produced lower values of C_e/C_0 (Figure 4b), however, T_{10}/T_{nc} was not a perfect predictor of pollutant removal ranking. For example, the greatest concentration reduction (lowest C_e/C_o) was achieved by C4.s1 and A2 (C_e/C_0 = 0.410±0.016 and 0.410±0.014, respectively), but these cases exhibited different T_{10}/T_{nc} = 0.47±0.02 and 0.55±0.03, respectively (Figure 4a). Further, the metric T_{10}/T_{nc} suggested that I1 was a top performer, but it only ranked in the middle quartile with regard to C_e/C_0 (= 0.454±0.014). This was because addition of so many islands significantly decreased the nominal residence time for I1 (42 s), relative to the open basin (63s), so that the benefit of removing the short-circuiting was offset by the loss of total water volume, which eliminated longer residence times and the removal potential they provide. This trade-off explained the occurrence of an optimum (minimum Ce/Co) topography volume between 1,000 and 1,500 cm^3, which corresponded to roughly 10% of the basin volume. That is, by adding a small amount of well-placed island topography, short-circuiting was reduced, which removed short times from the *RTD* that are associated with high pollutant concentrations at the exit. However, adding too much topography (here, g.t. 1,500 cm^3) reduced the nominal residence time of the basin, which eliminated longer times from the *RTD*, which would be associated with the most significant pollutant removal. While the idea an optimum topography volume is physically reasonable, we caution that the metric C_e/C_o was determined using a spatially-uniform uptake rate, whereas the introduction of spatially-varying depth and vegetation habitat might produce spatial variation in uptake rate, and this additional non-linearity might shift the optimum position.

Single Islands and Single Row of Islands

The single island configurations are represented by solid red symbols in Figure 4. In every case, the introduction of a single island at the inlet reduced short-circuiting (increased T_{10}/T_{nc}) and enhanced pollutant removal (reduced C_e/C_0), relative to the open basin. The greatest improvement with regard to short-circuiting was achieved by S3 (T_{10}/T_{nc} = 0.45±0.04), a single island occupying 1/3 of the basin width, which performed better than both narrower (S1, S5) and wider (S4) single islands. Moving the island farther from the inlet did not improve the performance. Specifically, S1 (island at inlet) and S2 (island shifted downstream by one island length) had the same performance, within uncertainty (Table 3). The addition of flanking islands (open red symbols in Figure 4) placed on either side of the central island generally improved the hydraulic performance (increased T_{10}/T_{nc}) relative to the single island without flanking islands (solid red symbols). For example, S1.s1 added flanking islands to S1, which increased T_{10}/T_{nc} from 0.39±0.02 to 0.46±0.02. The exception to this trend was S3 and S3.s1, for which T_{10}/T_{nc} was unchanged within uncertainty (Table 3). Flanking islands improved the water circulation in the following way. The central island split the inflow jet into two streams, and the flanking islands re-directed this flow into streamwise trajectories at 1/3 and 2/3 width of the basin, resulting in even flow across the basin width. Without the flanking islands, the flow deflected by the central island ran all the way to the sidewalls, creating streamwise flow concentrated near the walls, which was less uniformly distributed than the flanking island case and produced greater recirculation at the center. This difference is illustrated for S1 and S1.s1 in Figure 6. Given the positive benefits of flanking islands, additional cases considered the spacing between the central and flanking islands. Performance was improved with decreased distance between the islands. For example, compare topographies S5.s3 and S5.s4 (Figure 7). A decrease in island spacing between S5.s3 and S5.s4 increased T_{10}/T_{nc} from 0.36±0.02 to 0.50±0.02, and decreased C_e/C_0 from 0.52±0.03 to 0.432±0.006 (Table 3, Figure 4).

Cases with Multiple Island Rows

The hydraulic improvement associated with the island topographies was not correlated with the number of island rows (Figure 8), indicating that the specific placement of islands was more important than the number of islands. In designs with multiple rows, the addition of flanking islands in the first row improved hydraulic performance only for some designs. For example, compare C1A and C1A.s1. The addition of side islands in the first row increased T_{10}/T_{nc} from 0.43±0.07 to 0.57±0.03. Similarly, for case C3 the addition of side islands in the first row, creating C3.s2, increased T_{10}/T_{nc} from 0.47±0.02 to 0.54±0.04. However, within uncertainty, the addition of islands did not improve C4 or C5. Further, within uncertainty, the addition of first-row, side-islands did not reduce C_e/C_o in any of the cases (Table 3). To summarize, for cases with multiple rows, the addition of side-islands in the first row may reduce short-circuiting, but did not significantly change the potential for pollutant removal (C_e/C_o)

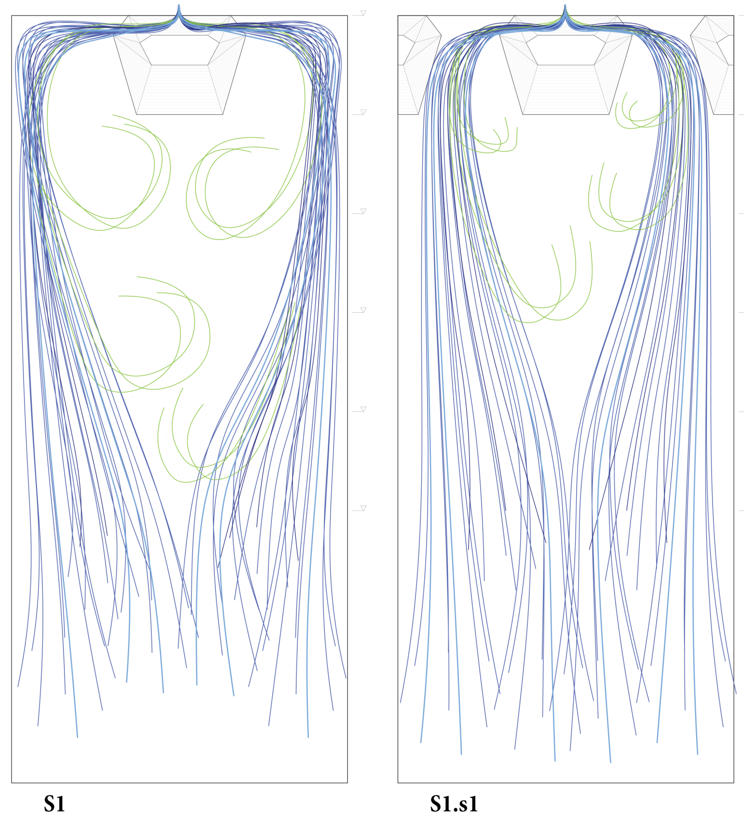

Figure 6. Circulation patterns for S1 with a single central island (left) and S1.s1 with flanking side-islands (right) based on digital tracer visualization. Blue lines indicate dominant flow lines. Green lines indicate recirculation zones.

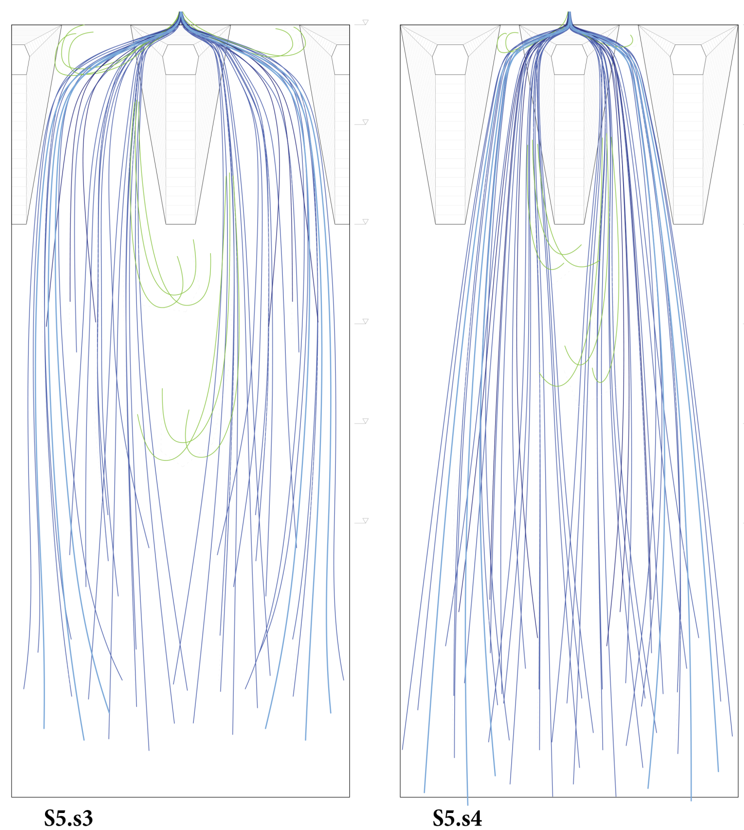

Figure 7. Circulation patterns for two cases with the same central island, but with flanking islands placed farther from center (S5.s3, left), and closer to center (S5.s4, right). Blue lines indicate dominant flow lines. Green lines indicate recirculation zones.

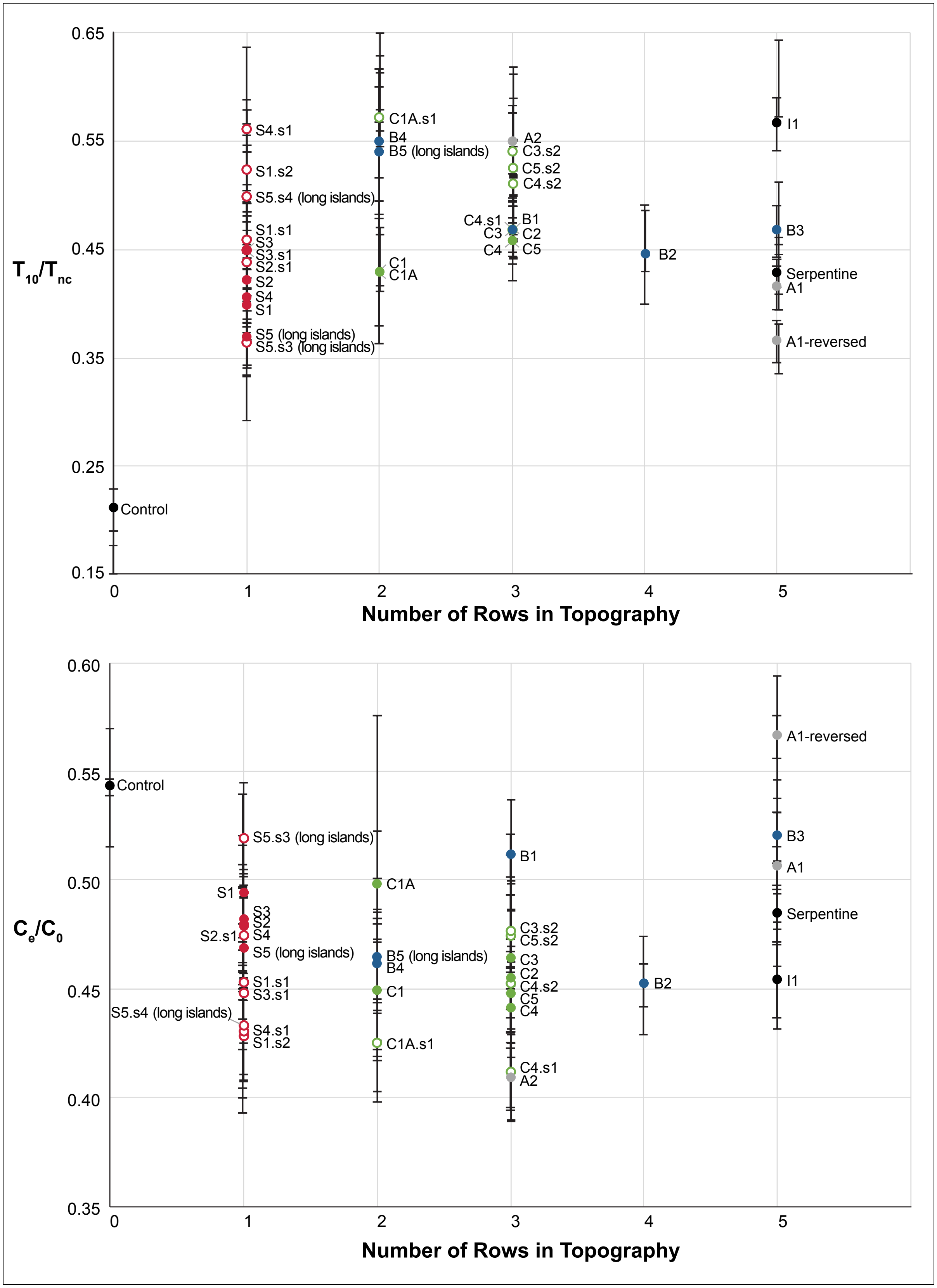

Figure 8. Performance metrics, (a) T_{10}/T_{nc} and (b) C_e/C_o, versus number of island rows. Error bars indicate 95% confidence interval based on two replicates and the propagated uncertainty in T_{nc}.

Streamlined Shape of Island

For most of the topographies the islands had a streamlined shape, i.e. the width of the island narrowed in the streamwise direction. A streamlined shape kept the flow from separating from the island, which was beneficial because flow separation creates recirculation and dead zones. The additional slope variation provided by the streamlined shape also contributed to emergent and submergent vegetative habitat. To confirm the hydraulic benefit of a streamlined shape, topography A1 was rotated 180° to create A1-Reversed, with the widest part of the islands closer to the inlet (Figure 2). The flow was distributed more uniformly across the basin width in A1, compared to A1-Reversed, in which the flow was directed away from the center and remained in more concentrated (narrower) flow streams (Figure 9). As a result, T_{10} was larger in the streamlined island case (A1), producing higher hydraulic performance (T_{10}/T_{nc} = 0.41±0.02), compared to A1-Reversed (T_{10}/T_{nc} = 0.36±0.02). Notably, A1-Reversed performed the worst of all cases in terms of the pollutant removal (C_e/C_0 = 0.566±0.010), and was significantly worse compared to A1 (C_e/C_0 = 0.506±0.010)

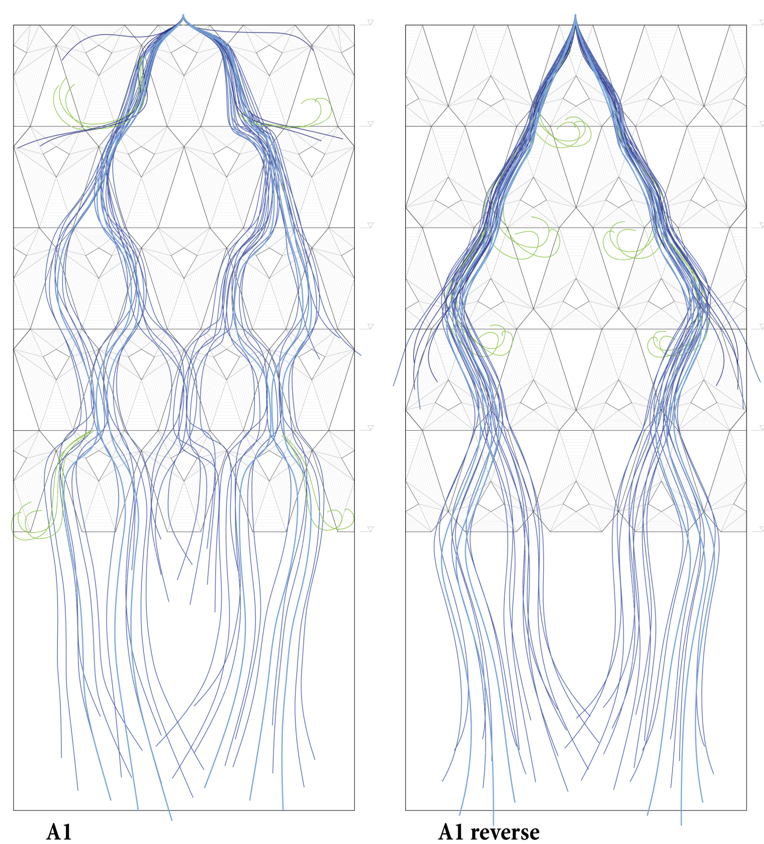

Figure 9. A comparison of flow lines for the streamlined-island case (A1, left) and the reversed-island case (A1-Reverse, right). The streamlined-islands spread the flow more uniformly across the basin width. The reversed islands direct flow away from center, creating a central dead zone that enhanced short-circuiting along the sides.

3.3 Construction Costs

The construction cost varied by only $454 across the 34 designs (Figure 10a), ranging from $7,369 (Serpentine) to $7,823 (A1). The costs were roughly equivalent for all designs because of the trade-off between excavation and island creation. Specifically, topographies with fewer islands required more excavation and less grading, while designs with more islands required less excavation but more grading. While the earthwork cost did not significantly differentiate between the designs, we caution that other costs not considered here, such as erosion control materials or maintenance, may create greater site specific differentiation.

3.4 Habitat Creation and Optimum Design

With 4 habitats, the maximum habitat diversity index was $H_{max} = 1.39$ (eq. 6). As shown in Figure 10b, the highest scoring design was I1 ($H = 0.99$), which had the largest island volume. The lowest index was for the control, which had a uniform water depth ($H = 0$). The serpentine design scored $H = 0.77$. As expected, the habitat diversity index increased with increasing island volume (Table 3), because larger (or more) islands contributed more surface area towards habitat differentiated from open water. At the same time, larger island volume did not necessarily improve hydraulic performance defined by the metric T_{10}/T_{nc} (Figure 4). By considering both habitat creation and hydraulic performance together (Figure 10b), the island topography I1 was shown to be the best option, providing both the greatest habitat diversity as well as one of the highest values of T_{10}/T_{nc}. Given that the cost variation was not significant (Figure 10a), this design may be the optimum choice amongst the cases considered here. However, I1 has the downside of providing the least water storage volume for a given water depth.

4. Conclusion

The first phase of this study established that a cluster of islands near the inlet provided the greatest improvement in the short-circuiting metric T_{10}/T_{nc}. In the second phase, 34 island clusters of greater topographic complexity were explored. All 34 designs achieved higher values of short-circuiting metric (T_{10}/T_{nc}) than the basin with no topography, and 23 achieved higher values than the conventional serpentine topography. The designs offer a range of habitat potential, with habitat diversity increasing with increasing island volume. For this reason, the optimum design in terms of the combined metrics of hydraulic performance (reduced short-

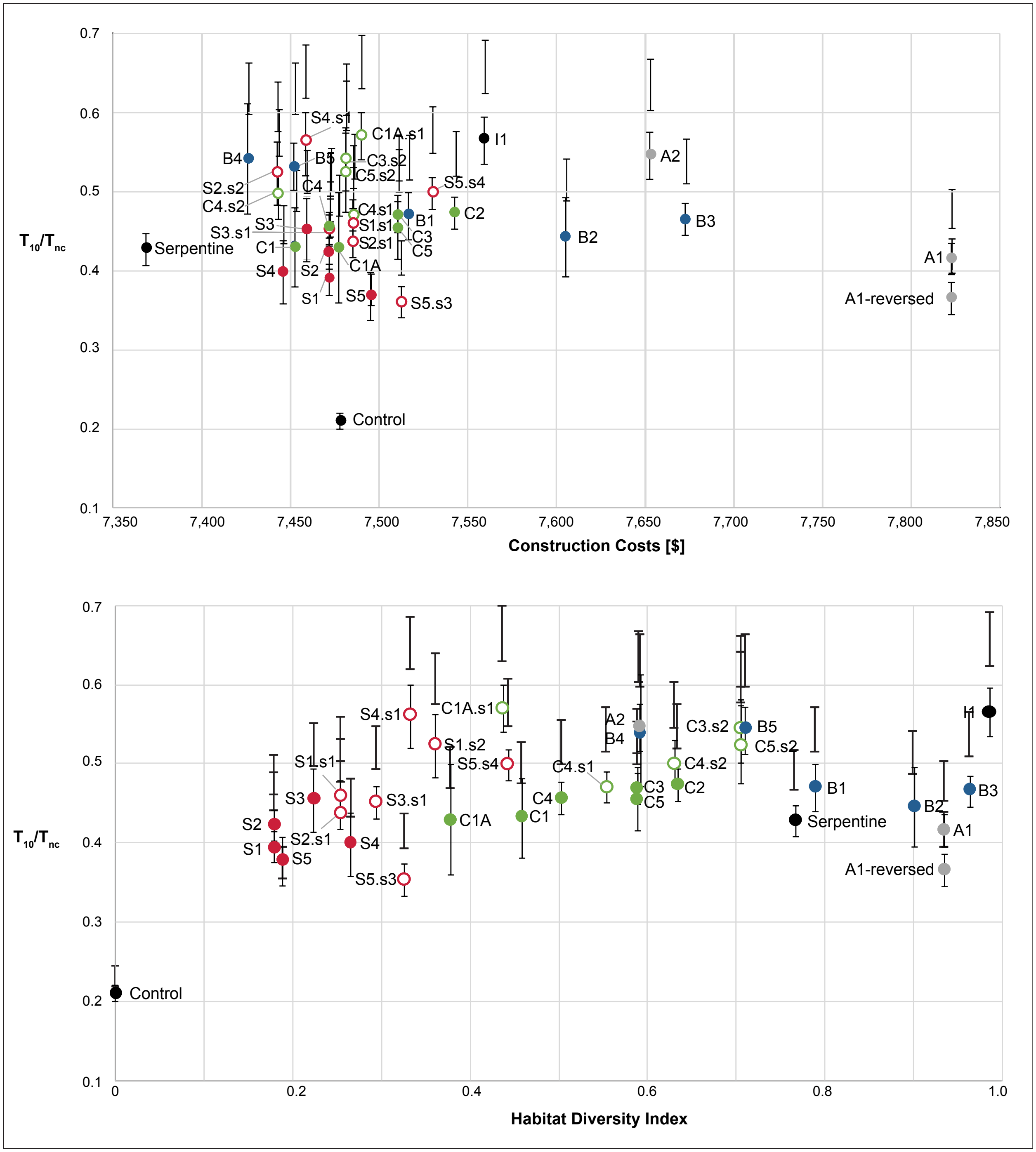

Figure 10 Comparison of (a) construction cost and (b) habitat diversity index across all designs. The error bars indicate 95% CI based on two replicates and the propagated uncertainty in T_{nc}.

circuiting) and habitat diversity was I1, a design with five rows of islands of decreasing size with distance from inlet. The construction costs did not vary significantly across the designs.

With regard to hydraulic performance alone, specifically the elimination of short-circuiting, designers have several options of high performing configurations with different amounts of topography (Figure 4). While it may seem that these complex island forms would be difficult to build, similarly intricate landscapes for multi-functional open spaces have been recently built in Europe. In Sweden, the MAX IV Laboratory is surrounded by a radial array of hills designed to dampen ground vibrations from the adjacent road (Snøhetta 2017). In Amsterdam, the Buitenschot Land Art Park includes a series of long, triangular mounds designed to reflect aircraft noise from the nearby Schiphol airport (H+N+S Landscape Architects 2017). New advances in construction technology, such as GPS controlled earthmoving equipment, render such complex landscapes increasingly feasible. To conclude, previous studies have encouraged an integration of engineering and ecology (Wurth,1996; Connor and Luczak, 2002). This study advanced the ecological basis for green infrastructure design by demonstrating the superior performance of several specific island cluster landscapes for improving both the hydraulic and ecologic function of detention ponds and treatment wetlands.

ACKNOWLEDGMENTS

This research was funded by a seed grant from the MIT Abdul Latif Jameel World Water and Food Security Lab from 2015 to 2017.

Cost Parameters			
	R.S. Means Unit Cost	Specifications	Cost
Excavation	31 23 16.46 Excavating, Bulk Dozer 2040 (page 294)	Using a dozer (80hp, 50’ haul) on an open site with clay soil.	$5.60 per cubic yard
Rough Grading: 2 passes	31 22 13.20 Rough Grading Sites 0170 8100-10000 S.F., dozer (pg 282)	Using a dozer on a site 8,100-10,000 square feet	$0.16 per sq. foot for each pass
Finish Grading: 1 pass	31 22 16.10 Finish Grading 2200 Slopes, Gentle (pg 282)	Using a dozer on a site 8,100-10,000 square feet	$0.21 per sq. yard for each pass

Table 1: Cost parameters use to estimate the earthwork cost, based on data from RSMeans (2017).

Table 2. Phase 1 testing results

Model	Solid Volume [%]	T_{10}/T_{nc}	$\delta(T_{10}/T_{nc})$
BER-1	15	0.25	0.03
BER-2	10	0.25	0.04
BER-3	15	0.31	0.04
BER-4	10	0.20	0.04
BER-5	10	0.29	0.05
ISL-1	10	0.17	0.03
ISL-2	15	0.13	0.04
ISL-3	10	0.17	0.04
ISL-4	15	0.14	0.04
CLU-1	10	0.51	0.05
CLU-2	10	0.23	0.10
CLU-3	10	0.20	0.04
CLU-4	10	0.38	0.04
CLU-5	10	0.18	0.04
CLU-6	10	0.20	0.05
CONTROL	0	0.22	0.06
PIN-1	NA	0.25	0.06
PIN-2	NA	0.18	0.03
PIN-3	NA	0.26	0.05
PIN-4	NA	0.24	0.05

Table 3. Hydraulic metrics T_{10}/T_{nc} and C_e/C_o for phase 2 topographies (Figure 2). Uncertainty (δ) is 95% confidence based on two replicates, as described in the *Methods*. The nominal residence time of the control had uncertainty δT_{nc} = 3s.

Topography	T_{10} [s]	δ T_{10} [s]	T_{nc} [s]	T_{10}/T_{nc}	δ (T_{10}/T_{nc})	C_e/C_0	δ (C_e/C_0)	Topography Volume [cm^3]	Diversity Index
A1	28.5	0.5	69	0.41	0.02	0.506	0.010	2980	0.93
A1-Reversed	22.5	0.5	62	0.37	0.02	0.566	0.010	2980	0.93
A2	35.5	0.5	65	0.55	0.03	0.410	0.014	1446	0.59
B1	28.0	0.5	60	0.47	0.03	0.511	0.010	2235	0.79
B2	32	3	71	0.44	0.05	0.452	0.010	2733	0.90
B3	29.0	0.5	62	0.47	0.02	0.520	0.012	2999	0.96
B4	35	4	62	0.55	0.07	0.46	0.04	1576	0.59
B5	35.5	0.5	66	0.54	0.03	0.46	0.02	2037	0.71
C1	28	3	63	0.43	0.05	0.45	0.03	1096	0.46
C1A	26	4	61	0.43	0.07	0.50	0.08	832	0.38
C1A.S1	34.5	0.5	61	0.57	0.03	0.42	0.03	1001	0.44
C2	30.0	0.5	63	0.47	0.02	0.454	0.006	1665	0.63
C3	32.0	0.5	68	0.47	0.02	0.464	0.004	1508	0.59
C3.S2	32.0	1.9	59	0.54	0.04	0.48	0.02	1988	0.71
C4	30.5	0.5	67	0.46	0.02	0.440	0.010	1227	0.50
C4.S1	33.5	0.5	71	0.47	0.02	0.410	0.016	1395	0.55
C4.S2	31.0	0.5	63	0.50	0.03	0.45	0.02	1707	0.63
C5	29.0	1.9	64	0.46	0.04	0.447	0.006	1508	0.59
C5.S2	34	3	64	0.52	0.05	0.48	0.04	1988	0.71
I1	35.5	0.5	63	0.57	0.03	0.454	0.014	3181	0.99
S1	25.5	0.5	65	0.39	0.02	0.494	0.004	323	0.18
S1.S1	27.5	0.5	60	0.46	0.02	0.45	0.02	491	0.25
S1.S2	34.0	1.9	65	0.52	0.04	0.429	0.014	803	0.36
S2	26.5	0.5	63	0.42	0.02	0.479	0.016	323	0.18
S2.S1	26.0	0.5	60	0.44	0.02	0.47	0.02	491	0.25
S3	27.0	1.9	60	0.45	0.04	0.48	0.02	436	0.22
S3.S1	29.5	0.5	65	0.45	0.02	0.45	0.02	603	0.29
S4	25.0	1.9	63	0.40	0.04	0.48	0.06	548	0.27
S4.S1	33.0	1.9	59	0.56	0.04	0.432	0.002	716	0.33
S5	26.0	1.9	68	0.38	0.03	0.47	0.02	337	0.19
S5.S3	22.5	0.5	62	0.363	0.019	0.52	0.03	674	0.33
S5.S4	31.5	0.5	63	0.50	0.02	0.432	0.006	1010	0.44
SERPENTINE	26.5	0.5	62	0.43	0.02	0.484	0.002	2148	0.77
CONTROL	13.5	0.5	64	0.210	0.013	0.54	0.04	0	0

REFERENCES

Adamsson, Å., L. Bergdahl, and M. Vikström. 2002. A Laboratory Study of the Effect of an Island to Extend Residence Time in a Rectangular Tank. In *Proceedings of the Ninth Internatinal Conference on Urban Drainage*, 1–10. Portland, Oregon: American Society of Civil Engineers. doi:10.1061/40644(2002)68.

Atkins, Inc. 2015. Flood Loss Avoidance Benefits of Green Infrastructure for Stormwater Management. U.S. Environmental Protection Agency, https://www.epa.gov/sites/production/files/2016-05/documents/flood-avoidance-green-infrastructure-12-14-2015.pdf.

Brandt, E., J. Petersen, J. Grossman, G. Allen, and D. Benzing. 2015. Relationships between Spatial Metrics and Plant Diversity in Constructed Freshwater Wetlands. *PLOS ONE* 10 (8): e0135917. doi:10.1371/journal.pone.0135917.

Connop, S., P. Vandergert, B. Eisenberg, M. Collier, C. Nash, J. Clough, and D. Newport. 2016. Renaturing Cities Using a Regionally-Focused Biodiversity-Led Multifunctional Benefits Approach to Urban Green Infrastructure. *Environmental Science & Policy,* 62 (August): 99–111.

Connor, M.A., and A. Luczak. 2002. Designing Wetland Treatment Systems That Contribute to Wildlife Conservation. In *Proceedings of the Eighth International Conference on Wetland Systems for Water Pollution Control*, 2: 1024–37.

Dewals, B., S. Kantoush, S. Erpicum, M. Pirotton, and A. Schleiss. 2008. Experimental and Numerical Analysis of Flow Instabilities in Rectangular Shallow Basins. *Environmental Fluid Mechanics,* 8 (1): 31–54. doi:10.1007/s10652-008-9053-z.

Dierberg, F., J. Juston, T. DeBusk, K. Pietro, and B. Gu. 2005. Relationship between Hydraulic Efficiency and Phosphorus Removal in a Submerged Aquatic Vegetation-Dominated Treatment Wetland. *Ecological Engineering,* 25 (1): 9–23. doi:10.1016/j.ecoleng.2004.12.018.

Dufresne, M., B. Dewals, S. Erpicum, P. Archambeau, and M. Pirotton. 2010. Experimental Investigation of Flow Pattern and Sediment Deposition in Rectangular Shallow Reservoirs. *Int. Journal Sediment Research* 25: 258–70. doi:10.1016/S1001-6279(10)60043-1.

Elmqvist, T., M. Fragkias, J. Goodness, B. Güneralp, P. Marcotullio, R. McDonald, S. Parnell, et al., eds. 2013. *Urbanization, Biodiversity and Ecosystem Services: Challenges and Opportunities*. Dordrecht: Springer Netherlands. doi:10.1007/978-94-007-7088-1.

Farjood, A., B. Melville, and A. Shamseldin. 2015. The Effect of Different Baffles on Hydraulic Performance of a Sediment Retention Pond. *Ecological Engineering,* 81: 228–32. doi:10.1016/j.ecoleng.2015.04.063.

Fogler, H. S. 1992. *Elements of Chemical Reaction Engineering*. Prentice-Hall, Englewood Cliffs, N.J..

German, J., and H. Kant. 1998. FEM-analys av strmningsförhållanden i en dagvattendamm (FEM-analysis of the hydraulic conditions in a stormwater detention pond). *Vatten* 54 (3): 183–90 (in Swedish).

Ghermandi, A., and E. Fichtman. 2015. Cultural Ecosystem Services of Multifunctional Constructed Treatment Wetlands and Waste Stabilization Ponds: Time to Enter the Mainstream? *Ecological Engineering,* 84: 615–23. doi:10.1016/j.ecoleng.2015.09.067.

Gómez-Baggethun, E., Å. Gren, D. Barton, J. Langemeyer, T. McPhearson, P. O'Farrell, E. Andersson, Z. Hamstead, and P. Kremer. 2013. Urban Ecosystem Services. In

Urbanization, Biodiversity and Ecosystem Services: Challenges and Opportunities, edited by T. Elmqvist, M. Fragkias, J. Goodness, et al., 175–251. Springer Netherlands. doi:10.1007/978-94-007-7088-1_11.

H+N+S Landscape Architects. 2017. Land Art + Soundscape, Buitenschot Park. http://www.hnsland.nl/en/projects/land-art-park-buitenschot.

Kadlec, R., and S. Wallace. 2009. Treatment Wetlands. 2nd ed. CRC Press, Boca Raton, FL.

Kearney, M., S. Fickbohm, and W. Zhu. 2013. Loss of Plant Biodiversity Over a Seven-Year Period in Two Constructed Wetlands in Central New York. *Environmental Management* 51 (5): 1067.

Khan, S., B. Melville, and A. Shamseldin. 2011. Retrofitting a Stormwater Retention Pond Using a Deflector Island. *Water Science & Technology* 63 (12): 2867–72. doi:10.2166/wst.2011.569.

Khan, S., and A. Shamseldin. 2013. Design of Storm-Water Retention Ponds with Floating Treatment Wetlands. *J. of Environmental Engineering* 139 (11): 1343–49. doi:10.1061/(ASCE)EE.1943-7870.0000748.

Krebs, C. 2009. *Ecology: The Experimental Analysis of Distribution and Abundance*. Pearson Benjamin Cummings, San Francisco, CA.

Lightbody, A., H. Nepf, and J. Bays. 2007. Mixing in deep zones within constructed treatment wetlands, *Ecological Engineering*, 29(2):209-220, doi:10.1016/j.ecoleng.2006.11.001.

Lightbody, A., M. Avener, and H. Nepf. 2008. Observations of short-circuiting flow paths within a constructed treatment wetland in Augusta, Georgia, USA. *Limnol. Ocean.,* **53**(3):1040-1053.Lovell, S., and D. Johnston. 2009. Designing Landscapes for Performance Based on Emerging Principles in Landscape Ecology. *Ecology and Society* 14 (1): 44.

Lovell, S., and D. Johnston. 2009. Designing Landscapes for Performance Based on Emerging Principles in Landscape Ecology. *Ecology and Society* 14 (1): 44.

RSMeans. 2017. Site Work & Landscape Costs. 36th ed. Robert S. Means Co., Kingston.

Moore, T. and W. Hunt. 2012. Ecosystem Service Provision by Stormwater Wetlands and Ponds – A Means for Evaluation? *Water Research*, Special Issue on Stormwater in Urban Areas, 46 (20): 6811–23.

Moore, T. and W. Hunt. 2013. Predicting the Carbon Footprint of Urban Stormwater Infrastructure. *Ecological Engineering,* 58: 44–51.

Persson, J., N. Somes, and T. Wong. 1999. Hydraulics Efficiency of Constructed Wetlands and Ponds. *Water Science and Technology* 40 (3): 291–300. doi:10.1016/S0273-1223(99)00448-5.

Persson, J. 2000. The Hydraulic Performance of Ponds of Various Layouts. *Urban Water* 2 (3): 243–50, doi:10.1016/S1462-0758(00)00059-5.

Rousseau, D., E. Lesage, A. Story, P.A. Vanrolleghem, and N. De Pauw. 2008. Constructed Wetlands for Water Reclamation. *Desalination* 218 (1–3): 181–89. doi:10.1016/j.desal.2006.09.034.

Savickis, J., A. Bottacin-Busolin, M. Zaramella, N. Sabokrouhiyeh, and A. Marion. 2016. Effect of a Meandering Channel on Wetland Performance. *J. Hydrology* 535: 204–10, doi:10.1016/j.jhydrol.2016.01.082.

Shannon, C., and W. Weaver. 1949. *The Mathematical Theory of Communication*. University of Illinois Press, Urbana, IL.

Shilton, A. 2001. Studies into the Hydraulics of Waste Stabilisation Ponds. Ph.D. Dissertation, Turitea Campus, Palmerston North, New Zealand: Massey University. http://mro.massey.ac.nz/handle/10179/2124.

Sleeper, B., and R. Ficklin. 2016. Edaphic and Vegetative Responses to Forested Wetland Restoration with Created Microtopography in Arkansas. *Ecological Restoration,* 34 (2): 117–23.

Snøhetta. 2017. MAX IV Laboratory Landscape. http://snohetta.com/projects/70-max-iv-laboratory-landscape

Taylor, J.R. 1997. An Introduction to Error Analysis: The study of uncertainties in physical experiments. 2nd Ed. University Science Books. ISBN-13: 978-0-935702-75-0

Thackston, E., F. D. Shields, and P. Schroeder. 1987. Residence Time Distributions of Shallow Basins. *J. Environmental Engineering,* 113 (6): 1319–32.

U.S. EPA. 2000. Guiding Principles for Constructed Treatment Wetlands: Providing for Water Quality and Wildlife Habitat. EPA 843-B-00-003. Washington, D.C. https://nepis.epa.gov/Exe/ZyPDF.cgi/2000536S.PDF?Dockey=2000536S.PDF.

U.S. EPA. 2015. Tools, Strategies and Lessons Learned from EPA Green Infrastructure Technical Assistance Projects. https://www.epa.gov/sites/production/files/2016-01/documents/gi_tech_asst_summary_508final010515_3.pdf.

U.S. EPA. 2017. "National Summary of State Information." *Water Quality Assessment and TMDL Information*. Accessed May 5. https://ofmpub.epa.gov/waters10/attains_nation_cy.control#prob_source.

Vivian-Smith, G. 1997. Microtopographic Heterogeneity and Floristic Diversity in Experimental Wetland Communities. *J. Ecology* 85 (1): 71–82.

Walsh, J. 2014. Chapter 2: Our Changing Climate. In *Climate Change Impacts in the United States: The Third National Climate Assessment*, edited by J.M. Melillo, T. Richmond, and G.W. Yohe, 19–67. U.S. Global Change Research Program.

Werner, T., and R. Kadlec. 1996. Application of Residence Time Distributions to Stormwater Treatment Systems. *Ecological Engineering* 7 (3): 213–34.

Wolf, K., C. Ahn, and G. Noe. 2011. Microtopography Enhances Nitrogen Cycling and Removal in Created Mitigation Wetlands. *Ecological Engineering,* 37: 1398–1406. doi:10.1016/j.ecoleng.2011.03.013.

Worrall, P., K. Peberdy, and M. Millett. 1997. Constructed Wetlands and Nature Conservation. *Water Science & Technology,* 35 (5): 205–13. doi:10.1016/S0273-1223(97)00070-X.

Wurth, A. 1996. Why Aren't All Engineers Ecologists? In *Engineering Within Ecological Constraints*, edited by P. Schulze, pp.129–40. Washington, D.C.: National Academies Press. http://www.nap.edu/catalog/4919.